Publishing House
AKAPIT

COMPUTER METHODS IN MATERIALS SCIENCE

Informatyka w Technologii Materiałów

Vol. 7, 2007, No. 2

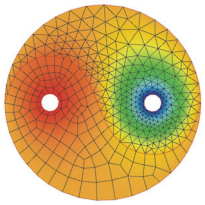

WEAK AND STRONG COUPLING OF SOLVERS IN PARTITIONED SOLUTION OF SOLIDIFICATION PROBLEMS

ARKADIUSZ NAGÓRKA

Częstochowa University of Technology, Institute of Computer and Information Sciences
ul. Dąbrowskiego 73, 42-200 Częstochowa, Poland

Abstract

In this paper a staggered scheme for partitioned solution of a coupled three-dimensional solidification problem is presented. Coupling is considered between several thermal and mechanical phenomena that take place in a mould and in a casting solidifying in the mould cavity. Numerical solution is based on the finite element method in space and the finite difference method in time. Two independently developed solvers are used for transient solution of non-linear heat and stress problems, respectively. Each solver solves its problem in the entire computational domain, which covers the casting and the mould, and is coupled with the other solver. The solvers can advance with different time steps and the coupling data is exchanged at selected times. Effects of weak and strong coupling of solvers are investigated. Numerical results show great influence of bidirectional coupling on the results when compared to the results of unidirectionally coupled run of the two solvers. In the weak case the solution scheme is explicit. The partial results of one solver are communicated to the other solver every selected number of time steps to be used in some further steps. Strong coupling makes the scheme implicit as it involves interfield iteration until convergence of results given by the two solvers is reached. This improves accuracy but increases computation time. Comparison of accuracy gain thanks to strong coupling to the improvement obtained by simply reducing time step size is also included in the paper.

Key words: partitioned solution, weak and strong solver coupling, contact, finite element method, solidification

1. INTRODUCTION

Many problems in science and engineering are described by systems of differential equations. Approximate solution of these equations can be obtained using discretisation methods such as the finite element method. If a discretisation method deals with all the equations at once, the solution is said to be *monolithic* as an algebraic system of equations is to be solved for all the unknowns at once. Sometimes it is possible to partition the system into subsystems which are dependent on each other through coupling variables. The subsystems (sometimes reduced to single equations) can be discretised independently and solved in a staggered way where a solver for a subsystem treats foreign coupling variables as load or boundary data.

This paper is devoted to such *partitioned* solution of thermomechanical phenomena taking place during solidification of castings. The coupling is bidirectional: temperature change causes thermal deformation, which leads to creation of air gaps on the interface between the casting and the mould. This results in change of intensity of heat exchange through the interface, hence the influence on the temperature.

2. MODELLING OF HEAT TRANSPORT AND DEFORMATION DURING SOLIDIFICATION

Consider a casting occupying the domain Ω_2 solidifying in a mould Ω_1, where $\Omega = \Omega_1 + \Omega_2$

ISSN 1641-8581

(see figure 1a). The casting is made of a two-component alloy and solidifies within a range of temperatures. Heat generation due to release of latent heat of phase change and heat transfer by conduction can be described by the heat equation in apparent heat capacity formulation (see, e.g. Dalhuijsen & Segal, 1986 and Ouyang &Tomma, 1996)

$$c^*(T)\frac{\partial T}{\partial t} - \nabla\cdot\left(\lambda(T)\nabla T\right) = 0 \quad \text{in } \Omega, \qquad c^* = \frac{\partial H}{\partial T} \quad (1)$$

where T the unknown temperature, c^* is apparent heat capacity, λ denotes heat conductivity and H is the enthalpy. Liquid-solid interface is not tracked explicitly as the latent heat is released in the volume of the mushy zone, defined as the region between solidus and liquidus isotherms where the solid phase fraction f_s is within the range from 0 to 1. The volumetric heat source is hidden behind the apparent heat capacity c^*. In this work the apparent heat capacity is piecewise linear in the range of solidification temperatures, which is a consequence of assumed piecewise parabolic approximation of the enthalpy in the mush. Also the solid phase fraction f_s is an explicit function of temperature.

Thermal deformation causes stress described by the equilibrium equations for $i, j = 1,2,3$

$$\sigma_{ji,j} + \rho(T)b_i = 0 \quad \text{in } \Omega, \qquad \sigma_{ij} = \mathrm{E}_{\mathrm{ijkl}}(\mathrm{T})\,\varepsilon^e_{kl},$$

$$\varepsilon^e_{ij} = \frac{1}{2}\left(u_{i,j} + u_{j,i}\right) - \alpha(T)\Delta T\delta_{ij} \quad (2)$$

where $\boldsymbol{u}$ is the unknown displacement, $\boldsymbol{\varepsilon^e}$ denotes elastic strain, $\boldsymbol{\sigma}$ is stress, ρ is density, $\boldsymbol{E}$ is elasticity tensor and α denotes linear expansion coefficient.

Galerkin finite element method was used to discretise the heat equation (1) in space, followed by application of the Euler backward finite difference method in time. Equilibrium equation (2) rewritten in an incremental form was also discretised by the Galerkin method. The solution was implemented in two distinct computer programs (solvers).

The stress solver is naturally coupled with the heat solver by the thermal loading term in equation (2). Simulating heat exchange across the interface involves an exchange coefficient. This is the place where coupling of the heat solver with the stress solver can happen. Local gap width g, being one of the results of stress analysis, can be used to evaluate the heat exchange coefficient k present in the interface boundary condition

$$\boldsymbol{q}_1\cdot\boldsymbol{n}_1 = -\boldsymbol{q}_2\cdot\boldsymbol{n}_2 = k\left(T_1 - T_2\right), \quad \text{where } k = \frac{1}{1/k_c + g/\lambda_g} \quad (3)$$

$\boldsymbol{q}$ is the heat flux, $\boldsymbol{n}$ denotes the outward unit normal, k_c is heat exchange coefficient of the protective coating and λ_g is conductivity of gas layer.

Temperature and solid phase fraction fields are computed by the thermal solver in each time step, possibly taking the gap width into account. Every selected number of steps the stress solver is given these fields to compute displacement, strain and stress increments caused by temperature change (see figure 1b).

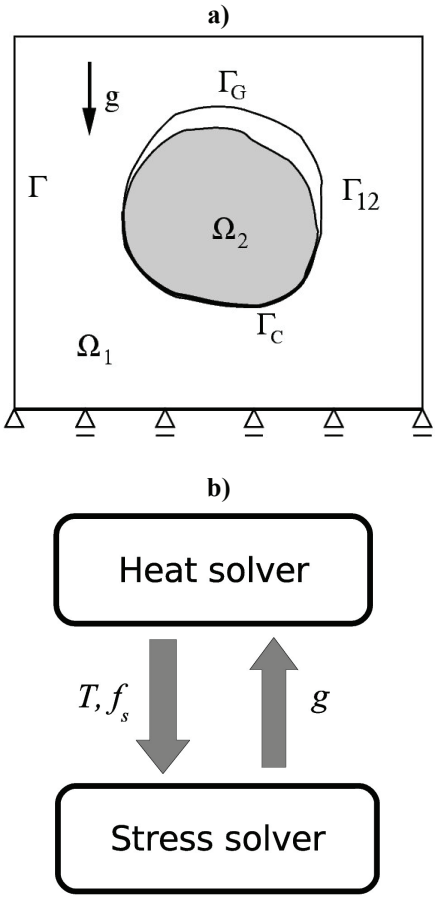

Fig. 1. *Contact between a mould and a solidifying casting (a) and coupling between the heat and stress solvers (b).*

Casting domain needs special treatment, as there is only liquid in the beginning. No special constitutive relation was assumed for the liquid. Finite elements occupied by the liquid are excluded from stress computations instead. They are subject to artificial elastic deformation, assuming small Young modulus, but the stress is kept equal to zero. It is the case until the element becomes partly solidified, that is until a threshold value of the solid fraction is reached within the element, provided that a crust of

such finite elements has formed around casting boundary. Stress in the crust is accumulated since then. The crust is detected by the analysis of the f_s field from the thermal solver.

Since weight and deformation of the casting has little influence on mould deformation, equilibrium equations are solved in two stages. First the mould is loaded by thermal increment field and deformation is calculated. Next the casting is deformed as the result on its thermal loading and also taking deformed mould configuration into account. If there is no crust yet, Dirichlet condition is imposed in the interface nodes to assure equal displacements of both nodes in each contact node pair. After the crust has formed, frictionless sliding condition is imposed in interface points, e.g. $\boldsymbol{x}_2$ in figure 2a, enforcing movement on a surface normal to the corresponding point $\boldsymbol{x}_1'$ on the preliminarily deformed mould. Namely, the displacement increment $\boldsymbol{\Delta u}_2$ must satisfy the condition

$$\boldsymbol{n} \cdot \boldsymbol{\Delta u}_2 - \boldsymbol{n} \cdot \left(\boldsymbol{x}_1' - \boldsymbol{x}_2 \right) = 0 \tag{4}$$

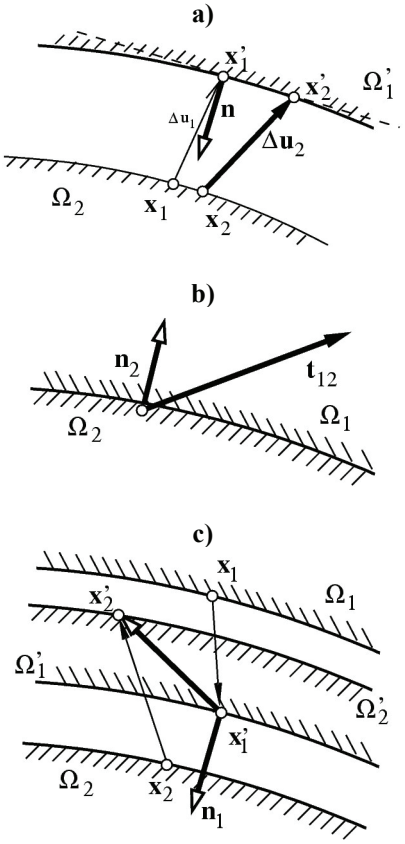

Fig. 2. Contact force, outward normal and displacements used in sliding condition on mould cavity (a) and in gap opening (b) and overlapping (c) criteria.

Stress solver analyses stress and displacement state along the interface. Knowing contact force makes it possible to detect tendency to create a gap in the part currently in sliding contact, namely the gap opens if $\boldsymbol{t}_{12} \cdot \boldsymbol{n}_2 > 0$, where $\boldsymbol{t}_{12} = \boldsymbol{\sigma}_2 \boldsymbol{n}_2$, as shown in figure 2b. If part of the interface is in the gap overlapping may occur. It happens if $\boldsymbol{d} = \boldsymbol{n}_1 \cdot \left(\boldsymbol{x}_2' - \boldsymbol{x}_1' \right) < 0$, where a comma means deformed mesh, as illustrated in figure 2c. If the condition is not satisfied, d is simply the gap width and the gap remains open in the considered point. In case contact state has changed on any element face of the casting-mould boundary, stress analysis is repeated in the new configuration.

Sliding constraints are imposed by the augmented Lagrangian method. The resulting linear systems with a zero block are solved iteratively using the Uzawa method. This allows to decouple linear solution for displacement degrees of freedom (a sparse direct method is used) from determining Lagrange multipliers (by simple matrix-vector multiplication). Details are given in (Nagórka & Sczygiol, 2006).

Reliable gap opening tests need accurate contact forces on the interface boundary. Such a force in the ith node can be interpreted as the surface traction and computed from the formula

$$\boldsymbol{t} = \boldsymbol{\sigma} \cdot \boldsymbol{n} \tag{5}$$

or as the nodal reaction given by

$$\boldsymbol{t} = \int_{\Omega_i} \boldsymbol{B}^T \boldsymbol{\sigma} \, dV - \int_{\Omega_i} \boldsymbol{N} \rho \boldsymbol{g} \, dV \tag{6}$$

(it is the normal component as the sliding is frictionless), where $\boldsymbol{B}$ is the matrix of basis function derivatives and $\boldsymbol{N}$ is the matrix of basis function values, as defined in (Zienkiewicz & Taylor, 2000), and Ω_i is the patch of elements containing the ith node. In the first approach nodal values of the stress and the outward normal are needed. It is troublesome, as in the finite element method stress is generally discontinuous across elements (e.g. piecewise constant for linear elements) and a smoothing procedure needs to be applied. Simple averaging (weighed average of values in adjacent Gauss points where derivatives are close to the exact values due to the so-called *superconvergence* of derivatives) works well inside the volume but is insufficient at boundaries, and this is the value at the interface boundary that matters most. More advanced stress postprocessing techniques, such as a variant of the superconvergent patch recovery method, would be necessary to obtain reliable boundary stress. The other ingredi-

ent in equation (5) also needs to be the result of some averaging of the outward normals on adjacent boundary faces. Thus the contact force evaluated from (5) is not reliable as the basis of gap tests. In the other approach nodal contact forces are computed as the volume integrals involving stress components, and during numerical integration only these highly accurate Gauss point values are considered. Therefore the gap opening test is based in this work on the forces evaluated using the formula (6).

If elements with linear basis functions are used in stress analysis, the strain is piecewise constant and the resultant stress is often distributed in checkerboard fashion. Stress components oscillate around the exact value and averaging of barycentre values would give pretty accurate nodal values. However, this constant-strain element cannot represent even linear distribution of thermal strain, which is the driving force calculated from temperature increment linearly interpolated over the element. Hence the idea of using second-order element with quadratic interpolation of displacement and piecewise-linear interpolation of strain and stress. A hierarchical quadratic element was used for representing displacement as it does not introduce extra nodes to the mesh and new degrees of freedom are associated with element edges. This allows to use the same mesh in thermal and stress analysis. A hierarchical basis introduced by Szabó and Babuška (1991) was adopted.

Gap creation test is executed on the face basis. The nodal contact force computed from equation (6) is interpolated in the centre of a boundary face and scalar product of this value and the normal vector is calculated. Doing the test in the centre lets avoid problems with ambiguity of the normal vector in a node. It could be average of normal vectors to the adjacent faces, either all or only those in contact, excluding gaps.

Imposing the sliding condition (4) if quadratic elements are used requires constraining not only nodal unknowns, but also the remaining hierarchical unknowns. In addition to nodal constraints (where edge unknowns are not involved), for each contact face an extra constraint in its centre is imposed, involving all the basis functions and the current normal to the corresponding mould face. The central point has the advantage that there is no ambiguity about the outward normal, unlike in contact nodes.

3. PARTITIONED SIMULATION

It is possible to solve the heat transport and the equilibrium equations in one computer program (solver). This monolithic approach involves algebraic equations with the vector of unknowns containing both temperature and displacement degrees of freedom, augmented with Lagrange multipliers. However, there are many reasons to partition the problem and solve each phenomenon using a distinct solver:

1) It is better from the software engineering point of view to develop and test the programs specialised for the selected phenomenon independently, as it was the case in this work. The thermal solidification solver is an extension to an existing general heat conduction solver. Similarly, the solidification stress solver is the result of specialisation of another solver for thermoelastic stress analysis.
2) Temporal discretisation of both phenomena in the monolithic approach would share the time step size, and possibly iterative solution would give all involved fields at once. However, the equilibrium equations are in fact quasi-static and since there is no explicit time variable in the formulation, the use of a time stepping scheme is not necessary.
3) Due to the fact that displacement is a vector quantity and temperature is a scalar, displacement unknowns and their matrix entries would dominate. Partitioning allows to take advantage of the fact that it is more efficient to solve two smaller systems of equations than one system of the size being the sum of the smaller sizes. Since the time of the solution of the algebraic equations for stress analysis dominates the time of thermal computations, it is possible to circumvent this disproportion by reducing the step size in temporal computations. As the result, stress can be advanced each specified number of thermal steps.
4) Another advantage of the partitioned approach is possibility to run the cooperating solvers on different processors or even on different machines connected by a network, which allows to solve bigger problems that would otherwise not fit in a single computer.

The simplest form of solver coupling is when the stress solver reads temperature files produced by the thermal solver, but the thermal solver is unaware of the air gap. In this *one-way* coupling case the entire thermal simulation can be run before the stress analysis is even started. The stress solver can read temperatures from each selected step and skip the steps between.

If the interface gap width is to be considered, the two solvers must cooperate. The thermal solver computes the temperature, then the stress solver reads it and computes the stress and the gap width, next the thermal solver reads the gap width and computes the temperature at the next time level etc. This is the simplest form of two-way coupling. Since a solver uses the previous step data from the other solver, the process is explicit and such coupling is said to be *weak* (Felippa et al., 2001).

If the other solver's data at the current time were available, it would be possible to improve accuracy. Although it is generally not the case, it is possible to use a predicted value of the coupling variable (e.g. roughly computed by the other solver), which results in an implicit method. Such *interfield* iteration involves exchanging data between the solvers until convergence occurs and is called *strong* coupling. Convergence tests can be done in both or in one of the solvers.

Thermal solver

```
for i := k, 2k, 3k,... do
  m := 0
  repeat
    m := m + 1
    wait for and read g_i^(m-1)   (2) (6)..
    for j := i-k+1,i-k+2,..,i do
      compute T_j^(m) and f_s,j^(m)
    end for
    save T_i^(m) and f_s,i^(m)
    signal the stress solver  (3) (7)
    if (weak coupling) then break
  until ||T_i^(m) - T_i^(m-1)|| / ||T_i^(m) - T_i-k|| < TOL
end for
```

Stress solver

```
for i := k, 2k, 3k,... do
  m := 0
  save g_i^(0) = g_i-k  (1)
  signal the heat solver
  repeat
    m := m + 1
    wait for and read T_i^(m) and f_s,i^(m)
                                   (4) (8)
    repeat
      compute u_i^(m), ε_i^(m) and σ_i^(m)
      detect gaps and overlaps
    until (contacts resolved)
    save g_i^(m)
    signal the heat solver  (5) (9)..
  until (heat solver done)
end for
```

Fig. 3. *An algorithm of bidirectionally coupled partitioned solution.*

In figure 3 an algorithm for partitioned solution of the solidification problem is sketched. Stress is computed every k thermal time steps. Numbers in parentheses indicate the order of wait/signal operations. A solver waits for notification that what it wants to read is available, then it reads the data, does its job, saves the results and notifies the other solver that the coupling variables are ready to use. The algorithm covers both weak and strong couplings. In the weak case the inner iteration stops immediately, whereas if the coupling is strong iteration proceeds until the relative correction of temperature (with respect to the temperature increment in this time interval) is smaller than a preassigned tolerance. The stress solver stops to iterate after the heat solver is finished. An exception is the time before a solidified crust forms, when the stress solver stops after one iteration (since there cannot be any gaps yet).

4. NUMERICAL EXAMPLE

A sequence of partitioned simulations of thermomechanical phenomena during solidification of an Al-Cu alloy solidifying in a metal mould were run in order to test the significance of introducing stress-to-temperature coupling and the efficiency of explicit and implicit coupling. A relatively simple casting-mould system was analysed as shown in figure 4a. This is actually a quarter of the real setting but it is sufficient to be analysed thanks to symmetry. An inflow and outflow of the melt is also neglected in the geometry.

The following initial temperatures were assumed: 960 K in the casting domain and 590 K in the mould domain. Robin boundary condition was imposed on external boundaries with the heat exchange coefficient 200 W/(m^{2}K) and ambient temperature 293 K. Interface boundary is the place of heat exchange with the coefficient 1000 W/(m^{2}K) and conductivity of gap air equal to 0.025 W/(mK). Many material properties of the casting and the mould were assumed to be temperature dependent, e.g. the Young modulus of the cast material was interpolated using the values 7,25 10^{10} Pa for 297 K,

$7{,}8\ 10^8$ Pa for 753 K, $2{,}5\ 10^8$ Pa for the solidus temperature equal to 886 K and 0 Pa for the liquidus temperature 926 K and above.

In addition to thermal loading, both casting and mould material are subject to gravitational loading (gravity acceleration points from top to bottom). Typical deformation of the casting and the mould after solidification has finished is presented in figure 4b. As expected, the solidified casting rests on the mould cavity and the air gap has pretty uniform width. However, character of mould and cast deformation is much more irregular during solidification.

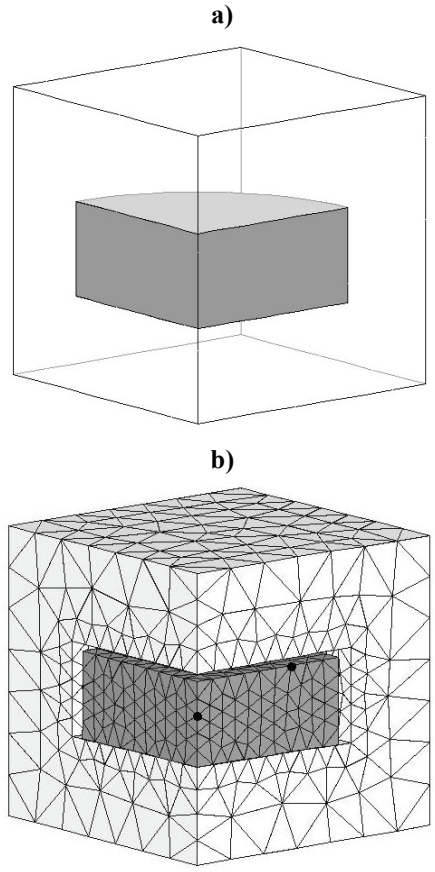

Fig. 4. *Geometry of the casting (grey) and the mould (white) (a) and the element mesh after deformation magnified 20 times (b).*

Test simulations were executed in the following settings

- one-way thermal-to-mechanical coupling with $\Delta t = 0.2$ s,
- two-way weak (explicit) coupling with $\Delta t = 0.2$ s,
- two-way weak coupling with $\Delta t = 0.1$s (half step size),
- two-way strong (implicit) coupling with two iterations per step,
- two-way strong coupling with the relative tolerance 0.001.

In all cases interfield data transfer was done every 10 time steps. In order to quantify accuracy, a reference solution was obtained with step size ten time smaller than usual, i.e. $\Delta t = 0.02$ s, and implicit interfield iteration done in every 10th step. Three iterations per such step were allowed. The result was assumed to be the „exact" solution to which the other results are compared. All the simulations were run on the *ACCORD* computational cluster in the Institute of Computer and Information Sciences at Częstochowa University of Technology. The series of simulations was run with both linear and quadratic tetrahedral elements for stress analysis (temperature computations were always done using linear elements). The results turn out to be practically the same, both in temperature and in stress, and will be illustrated once.

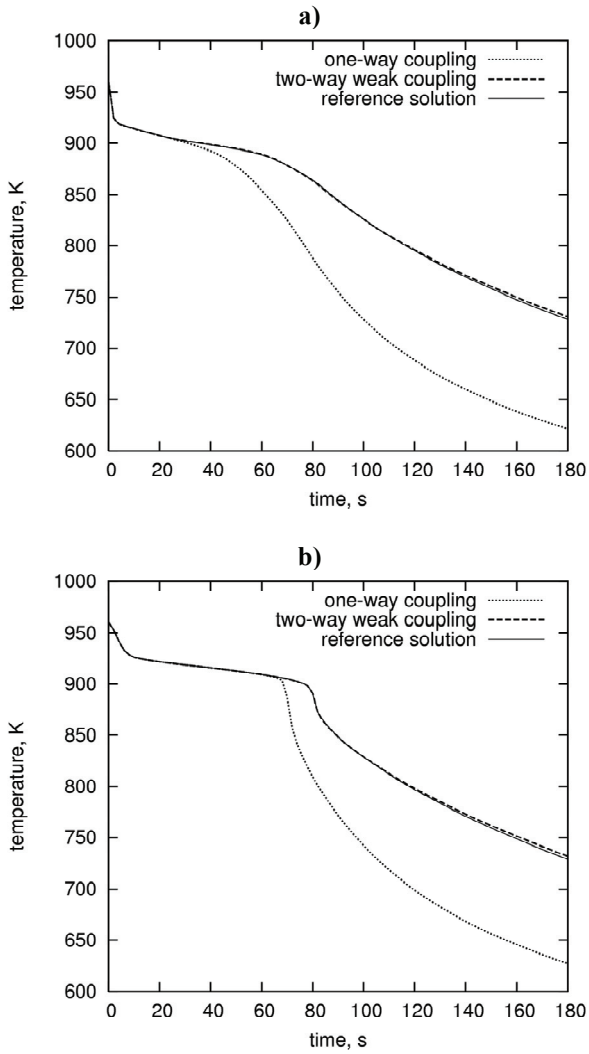

Fig. 5. *Variation of temperature in an interface node (a) and in a central node (b) for various types of coupling.*

Results of the simulations indicate great influence of mechanical-to-thermal coupling on the results, in addition to the usual thermal-to-mechanical coupling. Variation of the temperature in the selected nodes of the casting is presented in figure 5. The plots are given for the interface node and the central node

marked as black circles in figure 4b. Solid line shows the reference solution. Discrepancy between the reference solution and the solution with one-way coupling is huge, whereas even the simplest two-way coupling gives the solution with good agreement with the exact one. Results of one-way coupled simulation are of little value as it mispredicts the end of solidification by about 20 seconds. The curves start to diverge at the moment when stress begins to be accumulated in the casting. This is the time when solidified crust is formed around the casting boundary. The times are different in both figures because the cooling speed is faster close the interface (left) and slower in the centre of the casting (right).

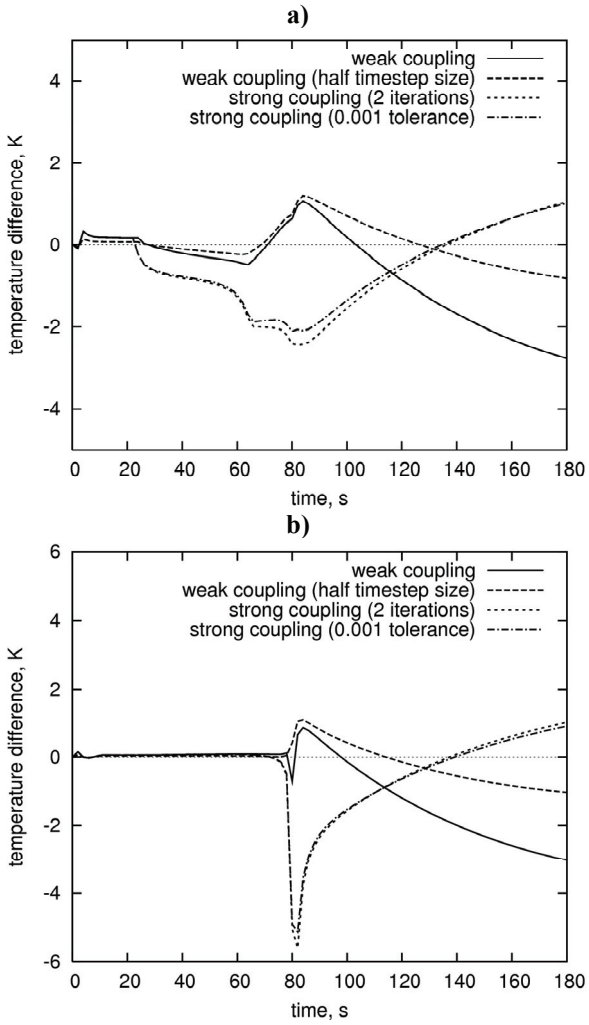

Fig. 6. *Variation of the error in temperature in the interface node (a) and in the central node (b) for various types of coupling.*

Table 1. *Convergence history at selected moments of a strongly coupled simulation*

Figure 6 shows the error in temperature in the selected nodes. The error is defined simply as the difference between a solution and the reference solution and is plotted for the two weakly (explicitly) coupled simulations and two strongly (implicitly) coupled simulations. Results of the simulation with unidirectional coupling were excluded as the error is much greater than a few degrees for these fully coupled computations. Analysis of the plots leads to a few conclusions. Firstly, halving the step size of explicitly coupled computations gives better improvement of accuracy than performing two implicit iterations (both approaches have the same computational cost). Implicit coupling with 0.001 tolerance gives only slightly better results but at much higher

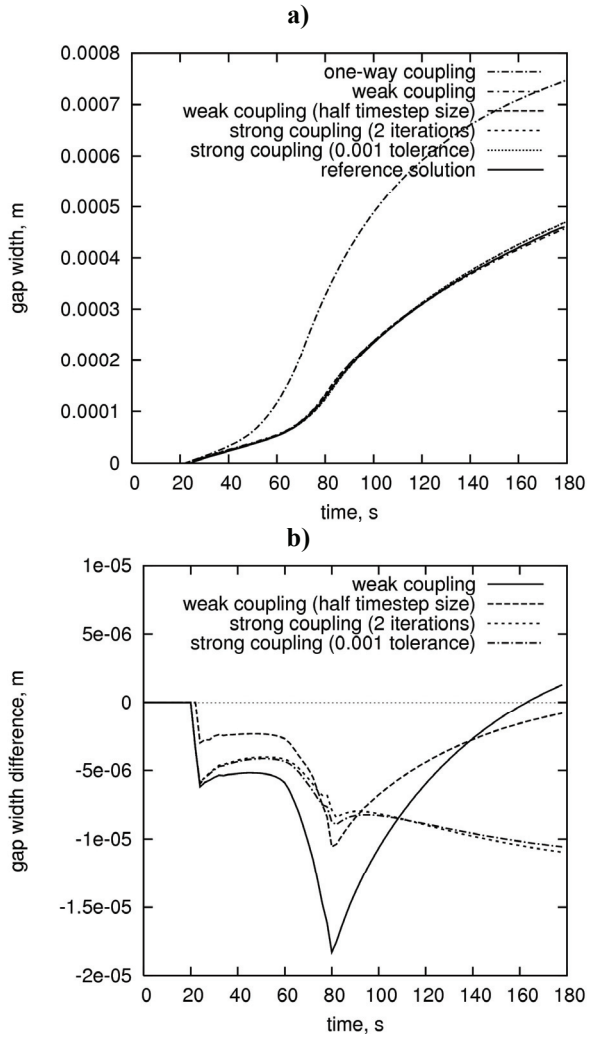

Fig. 7. *Variation of gap width (a) and gap width error (b) for the selected interface node.*

Iter.	Relative temperature correction									
	t = 30 s	t = 40 s	t = 50 s	t = 60 s	t = 70 s	t = 80 s	t = 90 s	t = 120 s	t = 150 s	t = 180 s
2	0.8625	0.5598	0.4715	0.5630	1.0308	0.7040	0.3234	0.0830	0.0456	0.0352
3	0.0675	0.0337	0.0255	0.0353	0.1149	0.1213	0.0273	0.0099	0.0035	0.0011
4	0.0053	0.0019	0.0012	0.0020	0.0117	0.0154	0.0067	0.0016	0.0005	0.0001

cost (the number of iteration per step is 4-5). Moreover, the error rises as the end of solidification approaches. This might be a consequence of modified backward Euler scheme used in time stepping, nonlinear iterations could improve efficiency.

In figure 7 variation of gap width in time in the selected interface node is illustrated. On the left side results obtained for various coupling types are compared with the reference solution. On the right side the error in gap width is plotted for the two explicit and the two implicit cases. Only the absolute error is presented, the relative error is much below 1%. The plots confirm the conclusion that it is better to reduce the time step of an explicit solution than to iterate implicitly.

In table 1 convergence of interfield iteration performed in the implicit (strong) coupling case is illustrated. Relative temperature corrections, defined as the L_2 norm of the difference between the temperatures from the two last iterations divided by the L_2 norm of the temperature increment (norms computed in the casting domain), are shown for consecutive iterations at selected moments in time. Convergence is excellent, it is however slightly slower at the time when solidification comes to an end, e.g. at $t = 80\,\mathrm{s}$.

5. FINAL REMARKS

According to Felippa et al. (2001), partitioned solution is preferred to the monolithic approach if coupling is local (e.g. through a surface, as in fluid-structure interaction problems) rather than global (through the volume, e.g. during plastic deformation of a metal piece). The thermomechanics of solidification studied in this paper is a problem that can be placed somewhere between, as thermal-to-mechanical coupling is volumetric and mechanical-to-thermal coupling is local (through the interface). Partitioned solution gives reasonably accurate results and lets avoid the shortcomings of the monolithic solution. However, there is still great disproportion between computational costs of thermal and mechanical solvers, even though the mechanical solver is called every selected number of thermal time steps. Stress analysis is more costly due to higher number of degrees of freedom (three unknowns per node as opposed to scalar temperature) and is elevated if higher-order elements are used. Solution of linear systems produced by finite element discretisation of the equilibrium equations is still a bottleneck. Plans are for speeding up the stress solver described in this work by introducing multigrid methods.

REFERENCES

Dalhuijsen, A.J., Segal, A., 1986, Comparison of finite element techniques for solidification problems, *Int. J. Numer. Meth. Engng*. 23, 1807-1829.

Felippa, C.A., Park, K.C., Fahrat, C., 2001, Partitioned analysis of coupled mechanical systems, *Comput. Methods Appl. Mech. Engrg*. 190, 3247-3270.

Nagórka, A., Sczygiol, N., 2006, Application of Lagrange multipliers to numerical solution of the problem of contact between thermally deforming bodies, *Proc. XIII Conf. KomPlasTech 2006*, eds, Szeliga, D., Pietrzyk, M., Kusiak, J., Szczawnica,111-118, (in Polish).

Ouyang, T., Tomma, K.K., 1996, Finite element simulations involving simultaneous multiple interface fronts in phase change problems, *Int. J. Heat Mass Transfer*, 39, 1711-1718.

Szabó, B., Babuška I., 1991, *Finite Element Analysis*, John Wiley and Sons, New York.

Zienkiewicz, O.C., Taylor, R.L., 2000, *The Finite Element Method*, Butterworth-Heinemann, Oxford.

SŁABE I SILNE SPRZĘŻENIE WSPÓŁPRACUJĄCYCH PROGRAMÓW OBLICZENIOWYCH W PODZIELONYM ROZWIĄZYWANIU ZAGADNIEŃ KRZEPNIĘCIA

Streszczenie

W pracy zaprezentowano dwustopniowy schemat podzielonego rozwiązania sprzężonego trójwymiarowego zagadnienia krzepnięcia. Rozważa się sprzężenie zjawisk cieplnych i mechanicznych zachodzących w formie odlewniczej i w odlewie krzepnącym we wnęce formy. Rozwiązanie numeryczne oparte jest na metodzie elementów skończonych w przestrzeni i na metodzie różnic skończonych w czasie. Dwa niezależnie rozwijane solwery (programy obliczeniowe) wykorzystane zostały do rozwiązania nieustalonych nieliniowych zagadnień transportu ciepła i analizy naprężenia. Każdy z programów rozwiązuje swoje zagadnienie w całym obszarze obliczeniowym, pokrywającym zarówno formę jak i odlew, i jest sprzężony z drugim solwerem. Poszczególne programy mogą wykonywać obliczenia z różnym krokiem czasowym, a dane sprzęgające są wymieniane w wybranych chwilach czasu.

W pracy bada się wpływ rodzaju sprzężenia solwerów na wyniki obliczeń. Rezultaty testowych obliczeń numerycznych wskazują na duży wpływ dwukierunkowości sprzężenia ciepło-naprężenia-ciepło w porównaniu ze sprzężeniem jednokierunkowym ciepło-naprężenia. W przypadku dwukierunkowym wyróżnić można sprzężenie słabe, w którym schemat rozwiązania jest jawny a wyniki przekazywane są drugiemu solwerowi co pewną liczbę kroków czasowych do wykorzystania w przyszłych krokach, oraz sprzężenie silne z niejawnym schematem obliczeń zawierającym proces iteracyjny, mający na celu uzgodnienie wyników dawanych przez obydwa współpracujące programy. Sprzężenie silne daje poprawę dokładności wyników, kosztem jednak większego nakładu obliczeń. W pracy pokazano również porównanie sprzężenia silnego i jego alternatywy w postaci sprzężenia słabego z mniejszym krokiem czasowym.

Submitted: October 10, 2006
Submitted in a revised form: December 7, 2006
Accepted: December 13, 2006